Combinatorial Biomolecular Nano-patterning for High-throughput Screening of Stem Cell Behavior

*Yacoub Y. I. Amin, Kasper Runager, Fabio Simoes, Adam Celiz, Vincenzo Taresco, Roberto Rossi, Jan J. Enghild, Lisbeth A. Abildtrup, David C. E. Kraft, Duncan S. Sutherland, Morgan R. Alexander, Morten Foss and Ryosuke Ogaki**

Supplementary Information

Experimental

Fabrication of nanopatterned platform: A clean 4-inch silicon wafer was spun coated with 4% methyl methacrylate, MMA (Micro resist technology GmbH) solution in a two-step spinning process at 500 and 5000 rpm for a total time of 60 s, obtaining a film thickness of around 45 nm. A 5.5% NXR-1025 thermal resist (Nanonex Inc.) was spun coated on top of the MMA using the same spinning process, yielding the film thickness of around 70 nm. The stamp and the resist-coated wafer were brought in contact and the patterns were transferred using a nanoimprinter (NX-2600, Nanonex Inc.) at 170°C for approx. 5 mins. Oxygen plasma (Advanced Vacuum) was used to etch the imprinted region with an O_2 flow rate of 100 sccm at 50 W to selectively expose the underlying silicon substrate. Physical vapor deposition equipment (Cryofox, Polyteknik A/S) was then used to deposit titanium (2 nm) and gold (10 nm) onto the substrate-exposed regions and the remaining resist was lifted off by sonication in acetone and isopropyl alcohol (IPA), and dried with a nitrogen flow. To generate the thick wells around the patterned regions, the gold/silicon nanopatterned wafer was first pre-baked at 200°C for 30 mins and SU-8 100 photo-negative resist (Microchem) was dispensed onto the wafer and spun coated in a two-step spinning process at 500 and 1100 rpm for a total time of 40 s. Soft baking of the wafer was carried out by heating the wafer on a programmable hot plate in a two-step heating process at 65 and 95°C for a total of 2 hrs. Once cooled, the photoresist coated wafer was aligned with a mask containing 128 patterned 9 mm^2 areas using a mask-aligner (EVG 610, EV Group) and subsequently exposed to UV at 650 mJ/cm^2. Post baking of the wafer was conducted by heating the wafer on the hot plate at 65 and 95°C for a total of 25 mins and the wafer is developed in EBR developer (MicroChemicals GmbH) solution, rinsed with IPA and MilliQ water and finally dried with nitrogen. The final well height was found to be around 300 μm. For generating unpatterned wafers, the fabrication was conducted from the PVD step onwards.

Parallel chemical nano-patterning of the platform: Oxygen plasma was first used to activate the SU-8 surfaces with an O_2 flow rate of 100 sccm at 50W. The activated wafer was sonicated in MilliQ water for 5 mins, rinsed and dried with a nitrogen flow. The wafer was incluated in a 2% (v/v) solution of 2-methoxy (polyethyleneoxy) propyl-trimethoxysilane (MPTS, Fluorochem Ltd.) were made in toluene and the wafer was incubated in the solution for 24 hrs under vacuum and subsequently sonicated in toluene, ethanol and MilliQ water for 2 mins each and dried with nitrogen.

Mixed thiol solutions (Prochimia) of biotinylated alkyl thiol (BAT) and methoxy-terminated tri (ethylene glycol) undecane thiol (OEG) were made by dissolving BAT and OEG in absolute ethanol and mixed in 1 to 9 molar ratios respectively with a total concentration of 0.1 mM. The silanized wafer was incubated in the BAT/OEG mixed thiol solution for 24 hrs and sonicated in ethanol for 2 mins and dried in a nitrogen flow.

*Combinatorial immobilisation of biomolecules:*Streptavidin solution at a concentration of 100 μg/ml in phosphate buffered saline (PBS) with 0.1% v/v glycerol was printed locally into each 9 mm^2 patterned area (3 μl each area) using an electronic multi-pipette dispenser (Multipette Stream, Eppendorf) and incubated in a highly humid environment for 2 hrs. The streptavidin printed wafer was rinsed by immersing in MilliQ water and dried in nitrogen. For ECM protein printing, mouse laminin 1 (Ln) and human vitronectin (Vn, Biotechne Ltd.) were first biotinylated using EZ-Link MicroSulfo-NHS-LC-biotinylation kit (Thermo Scientific) and desalting columns were used to remove the excess biotin. The level of biotin incorporation was found to be 8.6 ± 1.4 and 1.3 ± 0.2 (average ± standard deviation) biotin molecules per Ln and Vn molecules respectively, determined from 4´-hydroxyazobenzene-2-carboxylic acid (HABA) assay by measuring the change in the absorbance from HABA/avidin solution at 500 nm using a spectrophotometer (Nanodrop). The 8 different concentration ratios (w/v) of biotinylated protein solutions in PBS with 0.1% v/v glycerol were prepared at 100/0, 90/10, 80/20, 60/40, 40/60, 20/80, 10/90 and 0/100 (Ln/Vn), and printed onto streptavidin patterned areas in duplicates using an electronic multi-pipette dispenser and incubated for 2 hrs. Finally, the wafer was washed twice and stored in PBS before cell seeding.

Dental pulp stem cell isolation, culturing and cell seeding: The isolation and culturing of the human dental pulp stem cells (hDPSCs) were carried out by previously described methods[1] and in accordance to the guidelines approved by The Central Denmark Region Committee on Biomedical Research Ethics. Briefly, a third molar from a healthy young adult was surgically removed and the pulp was extracted from the molar and immediately incubated for 30 min at 37 °C in minimum essential medium (MEM, Gibco) containing 3 mg/ml collagenase type I (Worthington Biochem) and 2.4 units/ml Dispase II (Roche Diagnostics). The cell suspension from the pulp was strained and the isolated DPSCs were grown in a culture flask in MEM supplemented with 10% fetal bovine serum (FBS), 25.000 IU/ml pencillin and 25 mg/ml streptomycin. The combinatorial platform was first washed twice in PBS in a sterilized large petri dish and hDPSCs of passage 6 were seeded at a density of 10,000 cells/cm^2 in a serum-free condition (i.e. MEM only) and cultured for 4 hrs. The MEM was exchanged 2 hrs after seeding to remove any non-adhered cells.

Immunofluorescence for cell imaging and protein pattern visualization: The cell adhered platform was washed once in PBS, fixed in 4% paraformaldehyde and immersed in PBS with 0.1% v/v Triton-X 100 (T-PBS) for 15 mins. After removing the T-PBS, the wafer was incubated in 2% w/v bovine serum albumin (BSA) in T-PBS for 2 hrs, exposed to vinculin primary antibody at 1:800 (Sigma) for 90 mins and washed three times in T-PBS before being stained with a secondary antibody Alexa Flour 488 at 1:400 (Invitrogen) in T-PBS. Simultaneously, 4', 6-diamidino-2-phenylindole at 1:1000 (DAPI, Sigma) and rhodamine-labeled phalloidin (Sigma) at 1:400 (Sigma) in T-PBS were added to visualize nuclear fluorescence and actin cytoskeleton respectively and

incubated for 1 hr. The wafer was washed three times in T-PBS before image acquisition under the microscope.

For the visualization of the protein patterns, the protein immobilized platform was exposed to a 1:1 mixture of monoclonal primary antibodies of mouse laminin 1 antibody from rat (Biotechne Ltd.) and human vitronectin antibody from mouse (Biotechne Ltd.) with a total concentration of 4 μg/ml in PBS for 2 hrs and washed twice in PBS. The platform is then exposed to a 1:1 mixture of secondary antibodies of Alexa Fluor 568 goat anti-rat polyclonal IgG and Alexa Fluor 488 goat anti-mouse polyclonal IgG with a total concentration of 4 μg/ml in PBS for 2 hrs in darkness and washed twice in PBS before image acquisition.

Cell imaging and data analysis: The immunostained platforms were imaged using motorized Leica DM6000B microscope (Leica microsystems) with water immersion objectives. Two images from randomly chosen areas were acquired with ×10 magnification on each patterned 9 mm^2 area using a present stage moves and one representative image was manually acquired with ×63 magnification on each patterned 9 mm^2 area. Each acquired images were at least 0.5 mm away from the edge of the patterned area. Differential interference contrast (DIC), DAPI, red and green fluorescence images were recorded and transferred to the Leica IM500 database.

Data analysis was conducted from a total of 12 images per pattern/protein combination (n = 12) and all images were acquired with the patterns in parallel (0°) to the field of view and analyzed by ImageJ software (NIH). Color threshold was set manually for each image prior to image analysis. The cell number was determined by automatically detecting the positive DAPI stain per image and the average area per cell was calculated by first determining the total area of the cells from a positive actin image and dividing the total area by the total number of cells. The orientation of the cells were determined using Directionality plug-in in Image J Fiji software[2] from the actin images, a method which has been reported previously[3]. In brief, color threshold was manually applied to capture the outline of the cells from each actin image and all the images were automatically converted into binary images. The software employs 5 × 5 Sobel filter to detect the outline of the cells from the binary image and the software builds a histogram by recognizing the amount of image area with a preferred direction and separating the amount into a number of bins (9 bins were used in this study from -90° to 90° and the software reports the angle where 0° in the east direction and the orientation is counter-clockwise). Simultaneously, the software creates color maps for each image and these were manually checked against the color wheel with specified angles. Statistical analysis was conducted by expressing all the data with mean ± standard deviation. One-way analysis of variance (ANOVA) was performed using Origin 8 software (OriginLab) and the significant differences ($p < 0.05$) in the cell number and cell area between the patterned protein amounts for each pattern size were calculated using Bonferroni correction.

Surface characterization by scanning electron microscopy (SEM), time of flight secondary ion mass spectrometry (ToF-SIMS) and X-ray photoelectron spectroscopy (XPS):

SEM: Magellan 400 Field Emission Scanning Electron Microscope (FEI) was used to acquire all SEM images typically at an acceleration voltage of 5 kV, a nominal probe current of 50 pA with a working distance of 5 mm. For visualizing adhered cells on protein patterns, the cells were first fixed in 4% paraformaldehyde, then dehydrated by exposing the surfaces to a series of ethanol from 25% to 100% for 5 mins each step and dried with a nitrogen flow prior to SEM imaging.

ToF-SIMS: High resolution ToF-SIMS images were acquired with ION-TOF V (ION-TOF GmbH) in the high spatial resolution imaging 'burst-alignment' mode, using 25 keV Bi_1^+ primary ions rastered in a 256 × 256 (x,y) line format over a 50 μm × 50 μm area. The patterned surface was scanned in the high mass resolution 'high current bunched' mode to identify and confirm the secondary ions monitored in generating the secondary ion images in high spatial resolution with mass resolution (m/Δm) of better than 6000. All the acquired SIMS data was analyzed using Surface Lab 6 software (IONTOF GmbH) and the mass calibration was performed by selecting OH^- (m/z = 17), C_2H^- (m/z = 25) and C_4H^- (m/z = 49). For the characterization of SU-8 surfaces, positive ion spectra was recorded in high mass resolution in the same manner with electron flood gun and the spectra were calibrated to $C_2H_5^+$ (m/z = 29), $C_3H_7^+$ (m/z 43), $C_4H_9^+$ (m/z = 57) and $C_7H_7^+$ (m/z = 91).

XPS: For the silanization/thiolation control study on gold, XPS data was acquired using a Kratos Axis Ultra DLD instrument (Kratos Analytical Ltd) equipped with a monochromated Al kα X-ray source (hν = 1486.6 eV) operating at 10 kV and 15 mA (150 W). Survey spectra (binding energy (BE) range of 0–1100 eV with a pass energy of 160 eV) and high resolution C 1s and S 2p spectra were acquired and analyzed using CasaXPS (Casa software Ltd.) software. The BE scale for the high resolution spectra were calibrated by assigning C-C/C-H component in the C 1s spectra to the BE of 285 eV.

Relative quantification of surface bound proteins by liquid chromatography tandem mass spectrometry (LC-MS/MS): To analyze the laminin to vitronectin ratios on the surface of the nano-patterns each of the different protein ratios were incubated for 17 hours at 37°C with proteomics grade trypsin (Sigma) in 50 mM NH_4HCO_3 at a concentration of 30 ng/μL. The next day, the supernatant was recovered and the surface was washed once with 5 μL of 50 mM NH_4HCO_3. Digests from two areas were pooled for subsequent analyses. In order to reduce and block the thiols the combined sample was then incubated 30 min with 10 mM dithiothreitol followed by 60 min in the dark with 30 mM iodoacetamide. Prior to mass spectrometry analysis the peptides were desalted using POROS R2 resin (Applied Biosystems) and dissolved in 0.1% formic acid.

LC-MS/MS analyses were performed using an EASY-nLC II system (Thermo Scientific) connected to a TripleTOF 5600+ mass spectrometer (AB Sciex). The mass spectrometer was equipped with a NanoSpray III source and operated under Analyst TF 1.6.0 control. The trypsin cleaved samples were trapped on a Biosphere C18 column (Nano Separations) and eluted onto an analytical column from which they were eluted using a 20 min gradient from 5% to 35% phase B (0.1% formic acid in 90% acetonitrile). Area-based extracted ion chromatogram (XIC) quantification was set up as an

information-dependent acquisition experiment collecting 25 MS/MS spectra in each 1.6 s cycle using an exclusion window of 6 s.

All raw MS files were processed using Mascot Distiller 2.5.0 (Matrix Science). The MS data obtained by the analysis were processed using the default settings from the ABSciex_5600.opt file except that the MS/MS Peak Picking "Same as MS Peak Picking" was deselected and "Fit method" was set to "Single Peak". After peak picking all scans, a Mascot search was performed against the Swiss-Prot database (version 2015_01, 547,357 sequences). Carbamidomethyl modification of Cys residues was set as a fixed modification and biotinylation and proline oxidation were set as variable modifications. The data were searched with a mass tolerance of the precursor and product ions of 10 ppm and 0.2 Da. The default average [MD] quantitation protocol with a minimum peptide score of 30, number of peptides used for quantitation was 3, matched rho was 0.8, XIC threshold was 0.3 and isolated precursor threshold was set at 0.7. This label-free quantification protocol relies on the average MS signal response for the three most intense tryptic peptides for each protein. Data processing was performed in MS Data Miner v. 1.3.0.[4] The average relative protein amount and standard deviation was calculated for vitronectin and laminin-1 (gamma chain) from three samples and plotted in a histogram as molar ratios and with area-corrected ratios (Vn:Ln of 1:22, Fig. S4).[5]

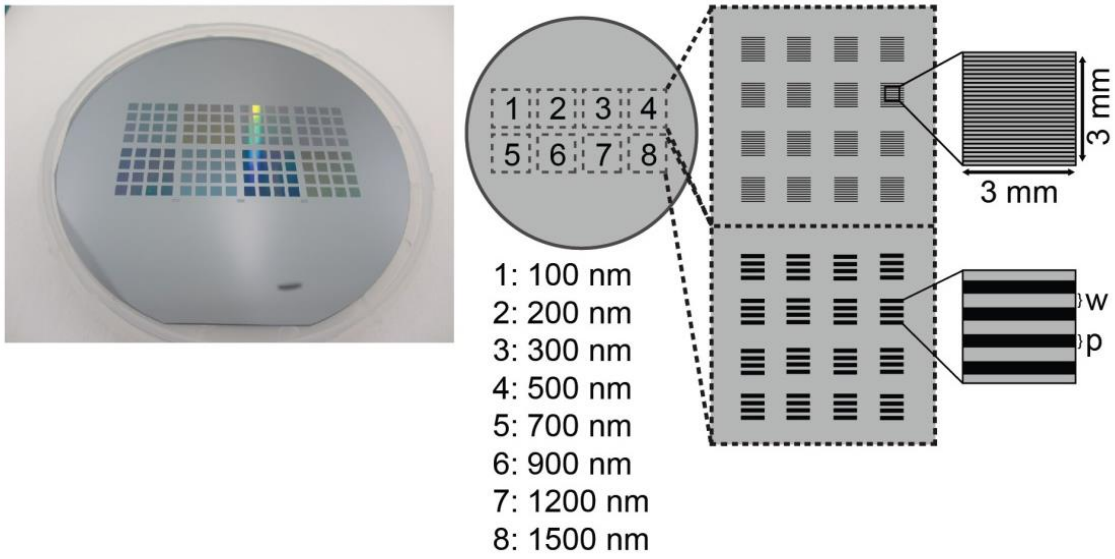

Figure S1: Stamp design for NIL. The stamp containing line patterns of equal width (*w*) to pitch (*p*) sizes from 100 – 1500 nm with the depth of 100 nm.

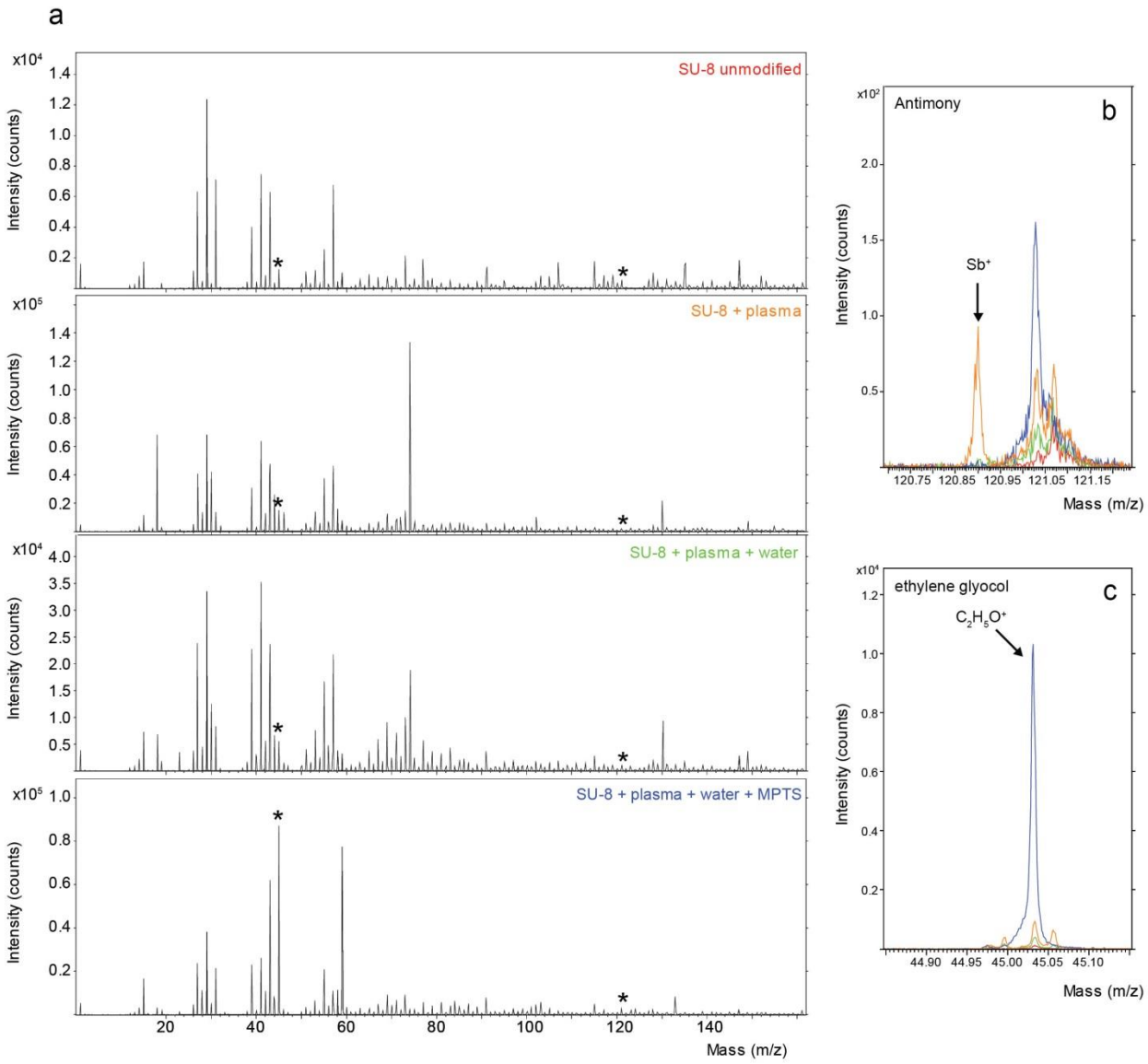

Figure S2: ToF-SIMS positive ion spectra of unmodified SU-8 (red), oxygen plasma treated SU-8 (orange), oxygen plasma and water treated SU-8 and MPTS grafted oxygen plasma and water treated SU-8 surfaces at m/z 0 – 180 (a). Asterisks indicate Sb^+ (b) and $C_2H_5O^+$ (c) secondary ions indicative of antimony from SU-8 and MPTS respectively.

The SU-8 surfaces required activation prior to chemical patterning in order to simultaneously render the Si regions and the SU-8 surfaces non-fouling by MPTS. Techniques such as oxygen plasma[6, 7] or UV/ozone[8] can be used to activate the SU-8 surface which will introduce oxygen-containing species for the subsequent silanization with MPTS. However, activation via high energy processes leads to accumulation of Antimony at the surface from the photo acid generator present in the SU-8 resist[7], which can be cytotoxic[9]. By sonicating the activated wafer in MilliQ water, Antimony at the interface can be successfully eliminated and grafted with MPTS, confirmed by the disappearance of Sb^+ signal at m/z 120.9 and increase in the $C_2H_5O^+$ signal at m/z 45.03 in the ToF-SIMS positive ion spectra.

	C 1s (%)	O 1s (%)	Si 2p (%)	Au 4f (%)	N 1s (%)	S 2p (%)
Bare Si	7.7 (0.3)	42.9 (0.5)	49.5 (0.6)	0	0	0
Si + MPTS	21.8 (0.3)	40.8 (0.3)	37.4 (0.3)	0	0	0
Si + MPTS + BAT/OEG	21.6 (0.2)	40.6 (0.2)	37.8 (0.3)	0	0	0
Bare Au	34.8 (1.4)	5.03 (0.6)	0	60.2 (1.7)	0	0
Au + MPTS	37.4 (0.8)	14.0 (0.6)	0	48.7 (0.8)	0	0
Au + MPTS + BAT/OEG	53.3 (1.0)	14.9 (0.4)	0	29.3 (0.5)	1.0 (0.3)	1.6 (0.1)

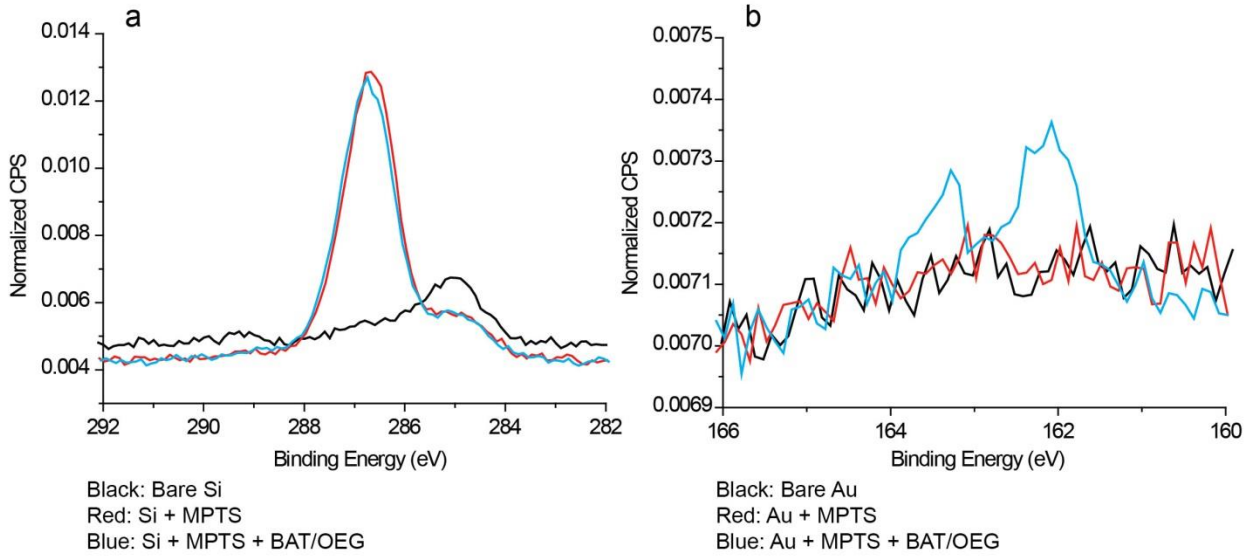

Figure S3: A table of relative surface elemental concentrations determined from XPS survey scans and high resolution XPS C 1s (a) and S 2p (b) spectra of Si and Au surfaces modified with MPTS and BAT/OEG.

The elemental scan and the C 1s spectra both confirmed the successful grafting of MPTS on Si, and the surface remained unchanged after the BAT/OEG exposure, where a dominant C-O peak can be observed at the binding energy (BE) of ~ 286.6 eV. A low level of MPTS adsorption was however observed upon exposure to the silane, highlighted by the reduction in Au 4f signal and the slight increase in the O 1s signal. Nevertheless, this did not hinder the subsequent BAT/OEG thiolation on Au, indicated by the successful thiolation, confirmed by the S $2p_{1/2}$ and $S2p_{3/2}$ peaks at the BEs of ~ 162 eV and ~ 163.2 eV, indicative of the gold-bound thiols[10].

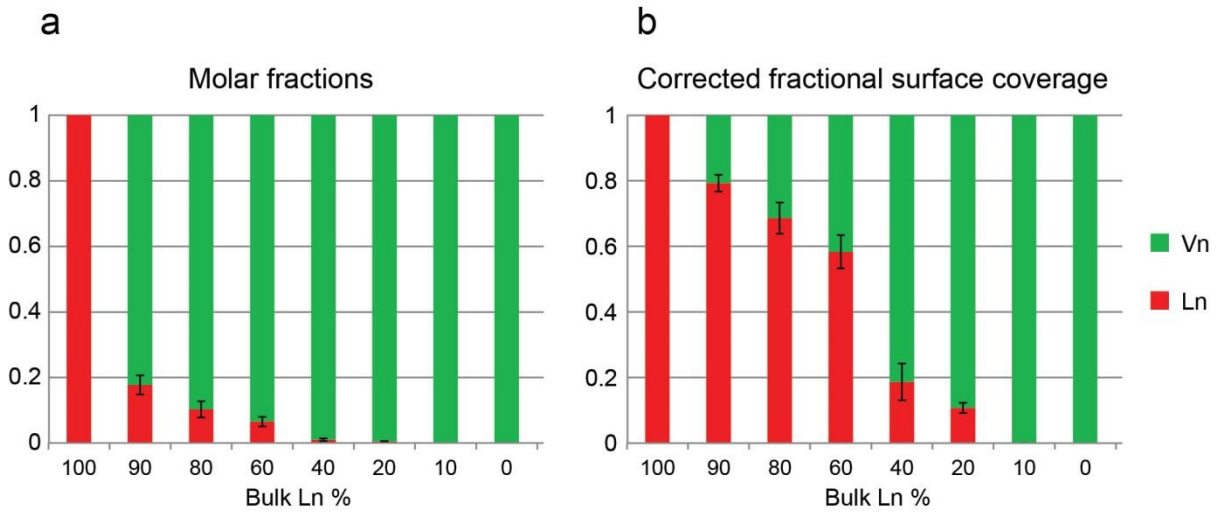

Figure S4: Relative molar (a) and corrected surface coverage (b) fractions of the laminin and vitronectin obtained from LC-MS/MS.

Relative quantification of surface bound ECM proteins by LC-MS/MS

Relative molar fractions were determined by first dispensing protein solutions onto the platform containing unpatterned surfaces (i.e. Au only) in triplicates and the surfaces were subsequently trypsinized and analysed using LC-MS/MS. The peptides from the laminin subunit γ1 and vitronectin were used to determine the relative molar fractions from the average intensities. A considerably higher amount of vitronectin was detected from the surface in comparison to the mixtures from the bulk (a). This was expected as vitronectin is considerably smaller than laminin, leading to faster rate of diffusion towards the surface. Laminin is expected to occupy approximately 22 times larger surface area (by assuming that the proteins are square in shape on the surface and the sizes of laminin and vitronectin are 70 nm and 15 nm in lengths respectively[5]) compared to vitronectin. The average fractional surface area coverage of the two proteins have been calculated by correcting the average intensities measured from laminin subunit γ1, confirming that the surface fraction of two proteins are relatively in good agreement with the bulk fraction. Note that the laminin signals could not be detected for the Ln 10% surfaces as the amount of laminin on the surfaces were below the detection limit of LC-MS/MS.

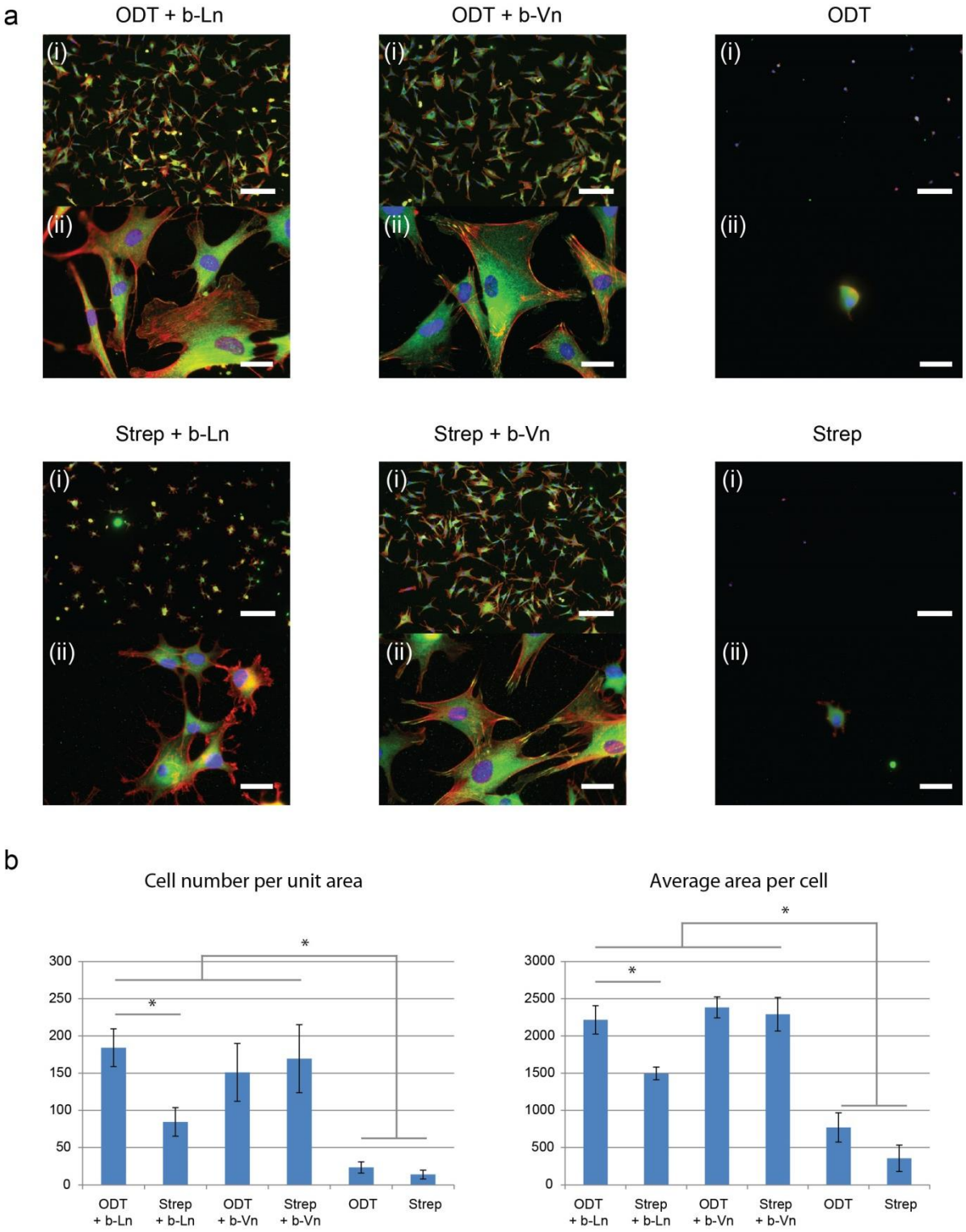

Figure S5: The representative ×10 (ai, scale bar = 200 μm) and ×63 (aii, scale bar = 30 μm) magnification images of the hDPSCs adhered on a variety of flat unpatterned surfaces including; biotinylated laminin (b-Ln) and vitronectin (b-Ln) physisorbed on hydrophobic 1-octadecane thiol modified gold surfaces (ODT + b-Ln and b-Vn); b-Ln and b-Vn immobilized via streptavidin on BAT/OEG modified gold surfaces (Strep + b-Ln and b-Vn); ODT modified gold surface (ODT) and

streptavidin on BAT/OEG modified gold surface (Strep). The cell number per unit area and average area per cell, μm^2 (b) are given (n = 12, $*P < 0.05$).

Discussion on the retention of protein conformation via affinity ligand based immobilization

We compared the adhesion behavior of hDPSCs on proteins immobilized via physisorption and affinity ligand interactions to determine whether the conformation of the proteins is retained by the immobilization method employed. Physisorption of biotinylated laminin and vitronectin (b-Ln and b-Vn respectively) were carried out by first incubating the clean flat gold surfaces overnight in 1-octadecane thiol, ODT (chemical modification confirmed by XPS, not shown), washed, dried in N_2 and subsequently exposed to biotinylated protein solution. Proteins are expected to denature upon interaction with a hydrophobic surface, mainly driven by hydrophobic interactions and irreversibly adhere onto hydrophobic surface, though the degree of denaturation is highly complex, determined by the intrinsic (i.e. properties of proteins, such as shape, size, charge domains determined by the amino acid sequence etc) and extrinsic parameters (i.e. temperature, pH, incubation time)[11]. After 4 hrs of culturing (with exchange of MEM after 2 hrs to remove non-adhered cells), higher average cell number and cell area were observed on the physisorbed laminin surfaces (ODT + b-Ln) compared to the laminin immobilized via BAT/OEG and streptavidin (Strep + b-Ln) as shown in Figure S5. The result strongly indicates that cryptic cell binding epitopes unfolded and exposed when laminins non-specifically adsorbed on ODT surface (e.g. the cell binding RGD sequence found in laminin 1 that is not accessible in its native form was exposed[12]) and the number of cell adhesion sites were increased on the surface, consequently allowing the cells to adhere and spread. In contrast, conformation of laminin was retained on Strep + b-Ln surface, resulted in having a lesser number of cell adhesion sites presented on the surface, leading to lower cell number and cell area. For the vitronectin modified surfaces, a statistically insignificant difference was observed of the cell adhesion behavior between the two types of surfaces (Figure S5b). This indifference in the cell adhesion behavior is most likely to be as a result of the cell-binding RGD sequence, which is found in vitronectin, are available regardless of whether the vitronectin is denatured or not. Cell adhesion behavior on ODT only and BAT/OEG + streptavidin only (Strep) surfaces were also investigated and it was found that the cells do not adhere nor spread favorably on these surfaces. In summary, based on the observations made from laminin immobilized surfaces and the confirmation of the presence of the laminin on the surface determined via immunostaining as shown in Figure 2c, our affinity ligand based immobilization approach retains the conformation of the proteins.

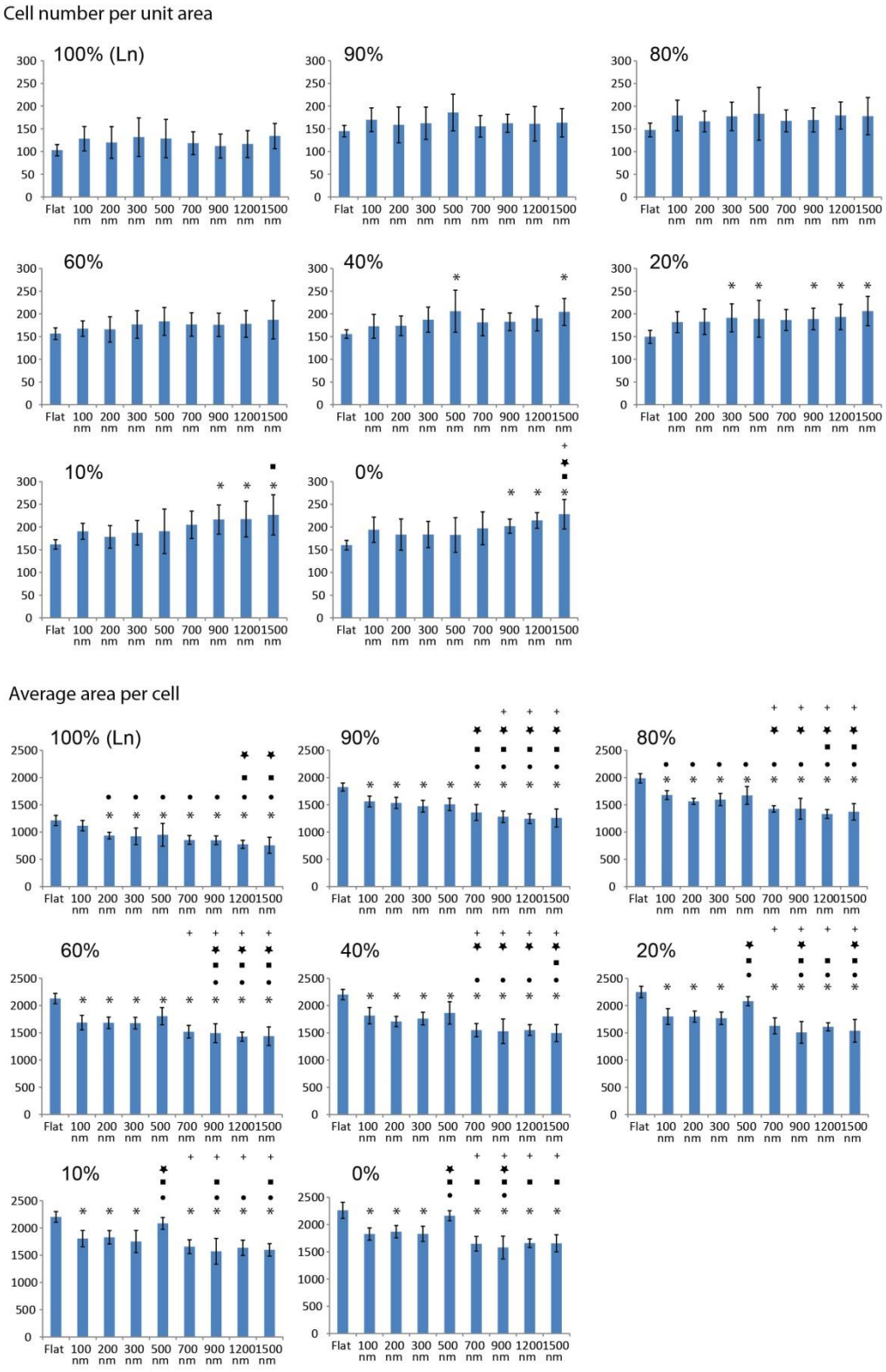

Figure S6: Summary of the cell adhesion data for cell number per unit area and average area per cell (n = 12 per combination). Y-axis represent cell number or cell area (μm^2) and X-axis represent bulk Ln %. $P < 0.05$ against Flat (asterisk), 100 nm (filled circle), 200 nm (filled square), 300 nm Ln (filled star) and 500 nm (cross).

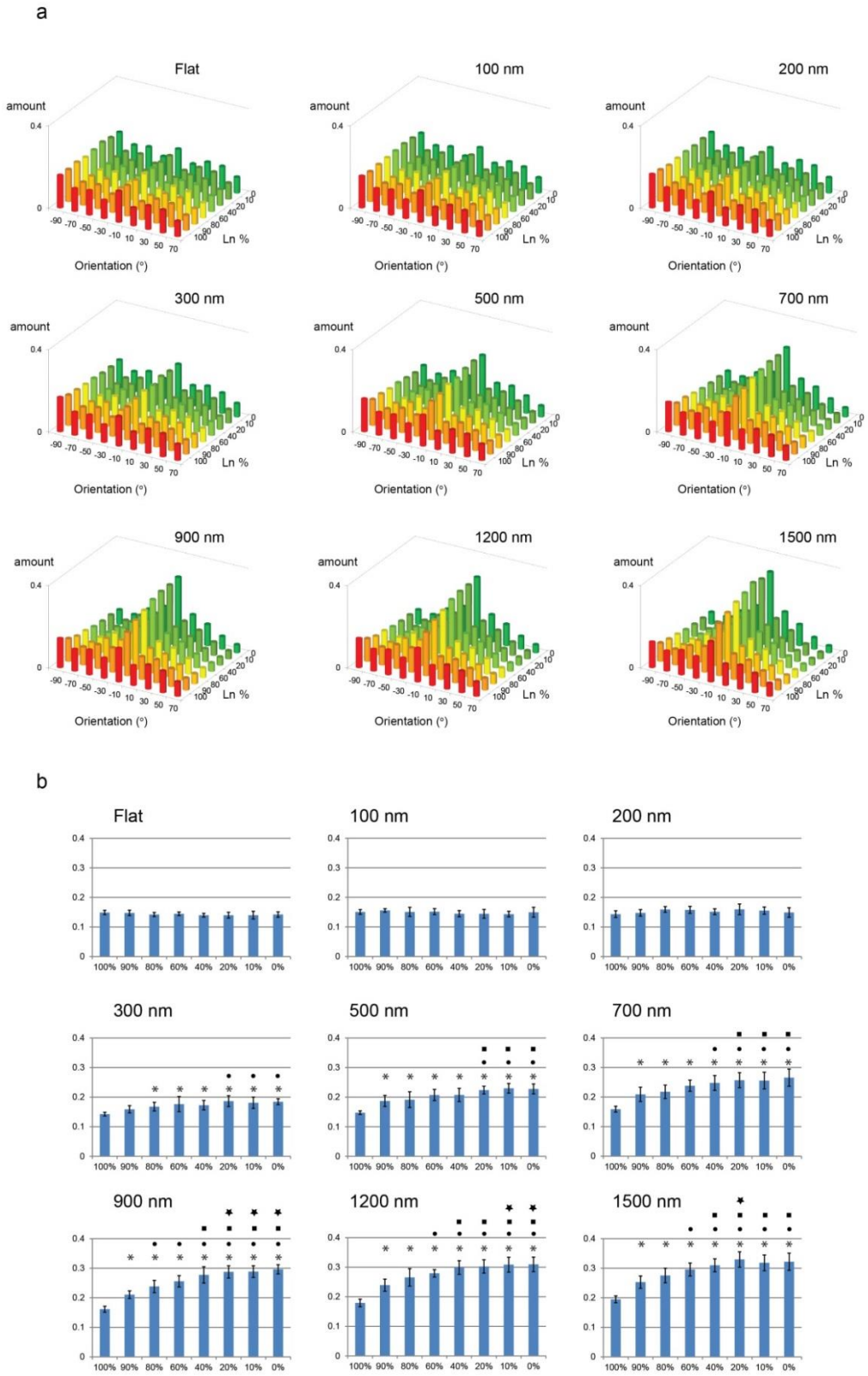

Figure S7: Orientation analysis of the adhered hDPSCs (n = 12 per combination). The entire dataset at angles of -90° to 90° (a) and the summary of orientation amount between -10° to 10° (b), where Y-axes represent amount and X-axis represent bulk Ln %. $P < 0.05$ against 100% Ln

(asterisk), 90% Ln (filled circle), 80% Ln (filled square) and 60% Ln (filled star). Details of oritentation analysis are given in online methods.

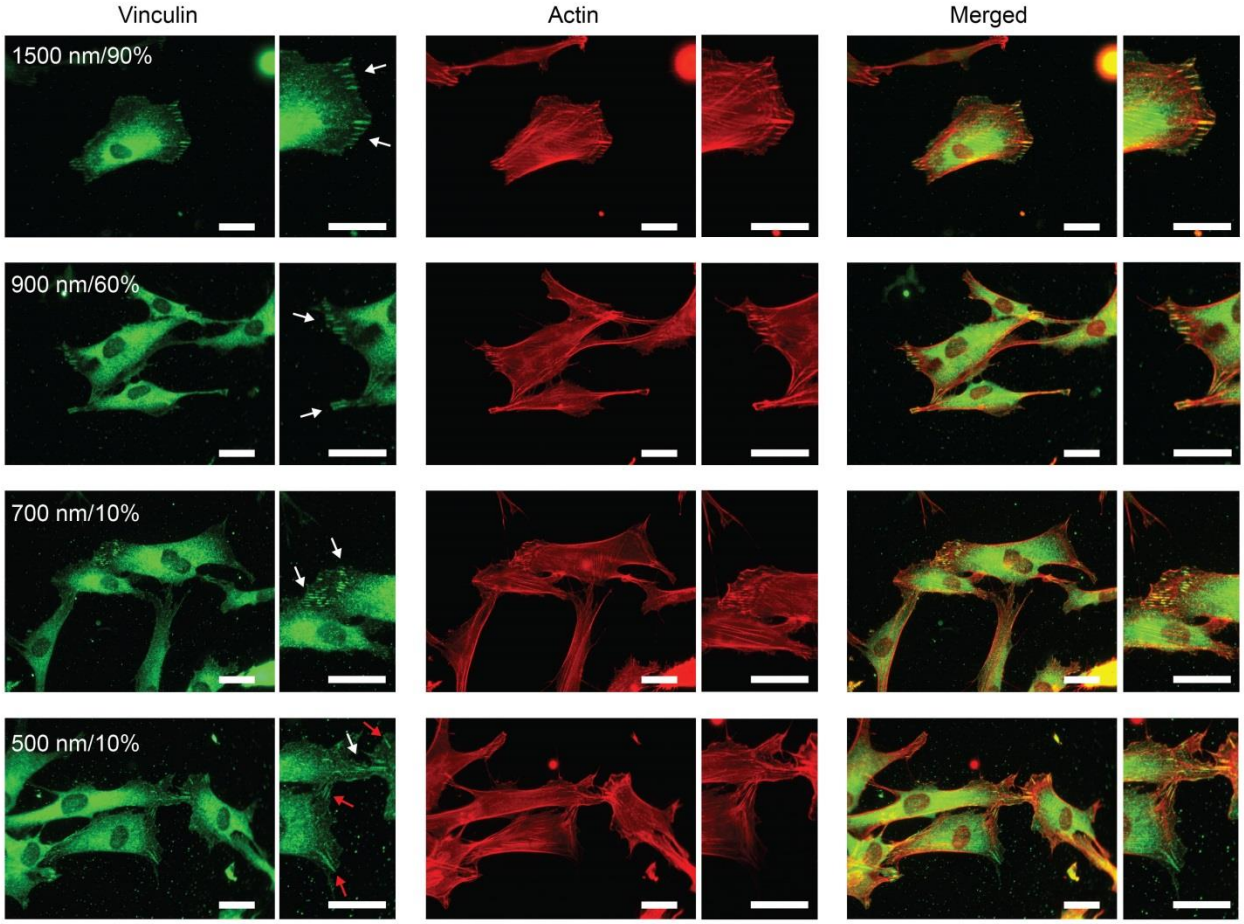

Figure S8: Higher magnification (×63) fluorescence microscopy images of hDPSCs on nanopatterned dual ECM protein surfaces. Scale bar = 30 μm. Digital zoom-in of the periphery of cells are given on the right hand side of each image.

The effect of nano-pattern size and surface protein ratio on cell area and orientation

We observed that at 100 and 200 nm, the cells were able to bridge the gap between the lines to spread in all directions thus resulting in low level of alignment to the line and the varying protein ratio did not have an effect on the cell alignment at these pattern sizes (Figure S7b). However increase in cell areas were observed with decreasing bulk Ln %, indicating that Vn is promoting cell spreading. The effect of varying surface protein ratios on alignment was observed for the pattern sizes ≥ 300 nm, where decrease in Ln % led to an increase in cell alignment. By analyzing vinculin and actin stained higher magnification images, the cells adhered on three different surfaces (1500nm/90% Ln, 900 nm/60% Ln and 700 nm/10% Ln) with statistically the same ($P < 0.05$) and high degree of alignment (orientation amount of ~ 0.26 at -10° to 10°) have typically shown

formation of long and distinct focal adhesions predominantly along the line pattern without bridging across the gaps between the lines (Figure S8, white arrows). By further comparing the cell adhesion behavior on 700 nm/10% with 500 nm/10% where Ln:Vn is the same, long focal adhesions were observed along the lines as well as bridged across the gaps between the lines predominantly on 500 nm/10% surfaces (Figure S8, red arrows). These results indicate that cells preferably exert force along the line for spreading when the pattern sizes are ≥ 700 nm, and the spreading was further promoted along the line by increasing in Vn amount, leading to an increase in the alignment but negligible change in the average cell area was observed. At 500 nm, cells were able to exert force along the line as well as across the line which resulted in having both high cell area and alignment. The protein type-dependent focal adhesion bridging across different nano-pattern sizes has been previously reported (comparing Vn to fibronectin, Fn) as a result of difference in the mechanical pliability of the protein (Vn being less pliable than Fn) leading to difference in exerted force and consequently affecting cell motility and spreading.[13] This may also be the case here where less mechanically pliable Vn compared to Ln supports higher force to be exerted to establish long and mature focal adhesions.

References:

[S1] D. C. E. Kraft, D. A. Bindslev, B. Melsen, B. M. Abdallah, M. Kassem, J. Klein-Nulend, European Journal of Oral Sciences 2010, 118, 29.

[S2] J. Tinevez, http://fiji.sc/wiki/index.php/Directionality 2010.

[S3] S. Fliegener, M. Luke, P. Gumbsch, Composites Science and Technology 2014, 104, 136.

[S4] T. F. Dyrlund, E. T. Poulsen, C. Scavenius, K. W. Sanggaard, J. J. Enghild, PROTEOMICS 2012, 12, 2792.

[S5] T. J. Webster, in *Nanostructured Materials*, Vol. 27 (Ed: J. Ying), Academic Press, 2001, 152.

[S6] W. Ferdinand, D. Polina, Z. Stefan, K. Michael, H. Helmut, M. G. Alexander, W. S. Robert, Journal of Micromechanics and Microengineering 2007, 17, 524.

[S7] F. Walther, T. Drobek, A. M. Gigler, M. Hennemeyer, M. Kaiser, H. Herberg, T. Shimitsu, G. E. Morfill, R. W. Stark, Surface and Interface Analysis 2010, 42, 1735.

[S8] L. E. Fissi, J.-M. Friedt, F. Chérioux, S. Ballandras, Sensors and Actuators B: Chemical 2010, 144, 23.

[S9] V. N. Vernekar, D. K. Cullen, N. Fogleman, Y. Choi, A. J. García, M. G. Allen, G. J. Brewer, M. C. LaPlaca, Journal of Biomedical Materials Research Part A 2009, 89A, 138.

[S10] R. Ogaki, F. Lyckegaard, P. Kingshott, ChemPhysChem 2010, 11, 3609.

[S11] D. G. Castner, B. D. Ratner, Surface Science 2002, 500, 28; B. Kasemo, Surface Science 2002, 500, 656; M. Rabe, D. Verdes, S. Seeger, Advances in Colloid and Interface Science 2011, 162, 87.

[S12] M. Pfaff, W. Göhring, J. C. Brown, R. Timpl, European Journal of Biochemistry 1994, 225, 975.

[S13] J. Malmström, J. Lovmand, S. Kristensen, M. Sundh, M. Duch, D. S. Sutherland, Nano Letters 2011, 11, 2264.